Slovak University of Technology in Bratislava
Faculty of Electrical Engineering and Information Technology

Ing. Martin Feiler

Dissertation Thesis Abstract

Photonic structures for sensor applications

to obtain the Academic Title of Philisophiae doctor (PhD.)

in the doctorate degree study programme: Electronics and Photonics

in the field of study: Electrotechnics

Form of Study: Full-time

Place and Date: Bratislava 20.7.2023

Dissertation Thesis has been prepared at the Institute of Electronics and Photonics, Faculty of Electrical Engineering and Information Technology, Slovak University of Technology in Bratislava.

Submitter: Ing. Martin Feiler
Institute of Electronics and Photonics
Faculty of Electrical Engineering and Information Technology
Slovak University of Technology in Bratislava
Ilkovičova 3, 81219 Bratislava

Supervisor: doc. Ing. Anton Kuzma, PhD.
Institute of Electronics and Photonics
Faculty of Electrical Engineering and Information Technology
Slovak University of Technology in Bratislava
Ilkovičova 3, 81219 Bratislava

Readers: prof. Mgr. Ivan Martinček, PhD.
Department of Physics
Faculty of Electrical Engineering and Information Technology
University of Žilina
Univerzitná 1, 010 26 Žilina

doc. Ing. Jozef Novák, DrSc.
Institute of Electrical Engineering
Slovak Academy of Sciences
Dúbravská cesta 9, 841 04 Bratislava

Dissertation Thesis Abstract was sent: ……

Dissertation Thesis Defense will be held on ..... at .....
at Faculty of Electrical Engineering and Information Technology, Slovak University of Technology in Bratislava, Ilkovičova 3, 81219 Bratislava

……
Prof. Ing. Vladimír Kutiš, PhD.
Dean of FEI of STU
Ilkovičova 3, 812 19 Bratislava

Contents

Introduction 3

Goals of the thesis 5

1 Brief state-of-the-art for waveguide-based SPR sensors 6

2 Simulation Methods 7

3 Design and simulations 10

3.1. Multi-mode waveguide-based refractive index sensor with a plasmonic layer 10

3.2. Single-mode waveguide-based refractive index sensor with a separated plasmonic layer 14

3.3. Design of the first iteration of the auxiliary circuit 17

3.4. Design of the second iteration of the auxiliary circuit 19

3.5. Near-field probes based on nanocone and nanopyramid structures 20

4 Fabrication 23

5 Characterisation 24

5.1. Coupling grating characterisation 24

5.2. Sensor characterization 26

Summary 28

Main results of the thesis 30

Resumé 31

References 35

Zoznam publikačnej činnosti 38

Introduction

Photonic technology is an indispensable part of the modern world surrounding us. Generally speaking, photonic technology consists of a source of light such as a laser or a LED and a waveguide to guide the light, e.g. fibre optics, and a variety of optoelectronic devices that encode digital signals onto optical ones, and consequently convert optical signals to electrical signals [1].

Things like high-speed telecommunication, the internet, light emitting diode (LED) lights, flatscreen TVs, CD and DVD players, driverless cars, laser-guided missiles, solar power, photonic-based sensors, and many others are more or less part of our everyday lives. Light-based technologies are efficient, reliable, and fast.

One of the fastest-developing branches of photonics is integrated photonics, in which waveguides and photonic devices are fabricated as one structure onto a substrate surface. Thanks to this integration, there is no need for optical interconnects between photonic devices, which allows complex photonic circuits to process and transmit light similarly to how electronic integrated circuits process and transmit electronic signals [2]. However, there are significant differences between electronic and photonic devices, which favour photonic circuits to replace conventional electronic circuits. While electrons are considerably slower and interact not only with one another but also with a conductor, which causes loss of power in the form of heat, photons are able to travel at a much higher speed with no interference, releasing only a fraction of the energy they carry [1, 3].

Among the most common applications of photonic devices is using optical radiation for sensing various parameters of materials, including material composition, refractive index, thickness, and many others. A huge focus in this field is on surface plasmon resonance (SPR), which has gone through extensive research in many theoretical and experimental studies for its ability to provide real-time sensing of various physical, chemical, or biological quantities [4, 5]. SPR sensors have been recognised as an up-and-coming platform for lab-on-chip bioanalytical sensing [6]. The underlying principle behind SPR sensors is a resonant oscillation of electrons at the metal-dielectric boundary of a sensor, resulting in a dip in reflectivity [7]. Various applications have

originated from the utilisation of this selective spectral attenuation, from Kretschmann and Otto configurations [8, 9], through waveguides, to fibre applications [5].

This work focuses on the design, simulation, optimisation, and analysis of the characterisation of various photonic structures and devices ranging from photonic sensors to passive components. Most of the devices and structures are based on the SiON material platform, chosen due to its characteristics like transparency in visible to mid-infra-red wavelengths, high thermal and oxidation resistance, and refractive index tunability, to name a few [10, 11].

Goals of the thesis

1. To obtain new knowledge in order to identify the most suitable methods for creating models of specific photonic structures for sensor applications.

2. To simulate optical parameters and characteristics of photonic structures and devices for sensor applications and optimise their properties for fabrication.

3. To design and simulate a model of plasmonic device based on SiON material for sensor application using appropriate simulation methods.

4. To analyse optical and structural properties, such as efficiency and sensitivity, of fabricated SiON waveguiding structures.

1 Brief state-of-the-art for waveguide-based SPR sensors

Optical sensors are widely used for refractive index measurements across many fields, including the biomedical and food processing industries. Due to specific field distribution and changes in light's intensity, phase or resonance wavelengths, these sensors might offer high sensitivity to ambient refractive index variation [12]. Various applications have originated from the utilisation of this selective spectral attenuation, from Kretschmann and Otto configurations [8, 9], through the waveguide, to fibre applications [5]. In the case of the Kretschmann/Otto configuration, extensive research brought even better sensitivity and selectivity by introducing various stacked metal or dielectric layers complimenting basic metal nano-film [13–15]. However, while SPR sensors based on Otto or Kretschmann configurations are usually unfit for integration due to their size or the necessity to use a prism coupling for SPR, waveguide-coupled SPR sensors provide suitable alternative thanks to their ease of use, significantly smaller footprint, and suitability for integration with other photonic components and sensors while theoretically maintaining sufficient sensitivity [16].

Since the early 90s, when waveguide-based SPR sensors were first introduced [17-19], they have undergone extensive research in terms of applications, design, sensitivity improvement, etc. Various configurations and material platforms have been introduced, each boasting its own advantages and unique characteristics. The most commonly used material platforms were either CMOS-compatible ones such as silicon [6], silicon carbide[15] and doped silica [20] or polymers [21] due to their fabrication simplicity and low cost. Even though single-mode waveguide-based SPR sensors are generally the most commonly used while promoting excellent sensitivity [21], other configurations, such as combined multi-mode platforms[20, 22] or combined amplitude and phase sensors [23], have been presented. These other configurations usually offer more robustness and bigger numerical aperture for incoherent optical sources [20], as is the case of planar multi-mode waveguide-based sensors, or offer improved sensitivity via more complex structures.

2 Simulation Methods

Computer simulation methods play an essential part in the design of new photonic devices and their subsequent optimisation. It is a crucial step preceding fabrication, which helps decrease the cost and complexity of the design and fabrication of photonic devices. The numerical and simulation methods presented in this chapter are included in RSoft Component Design [24] suite and its modules, which were chosen as a simulation program for the needs of this research. RSoft Component Design suite is used to define the most important input parameters required by simulation modules. These include material properties and structural geometry of photonic circuits. The start of the workflow for the user is designing the structure in a Computer-Aided Design (CAD) environment, followed by using one or multiple simulation modules for simulations of different performance aspects of devices and circuits. Thanks to RSoft CAD, individual modules are connected on the level that ensures continual work with the same devices throughout different modules.

Beam Propagation Method

The Beam Propagation Method (BPM) is a technique using the finite difference method to obtain numerical solution of Helmholtz equations. This numerical method allows the longitudinal grid (i.e. along the *z*-axis), for many applications and devices, to be much coarser than in the case of other commonly used numerical methods. It is one of the contributing factors to the BPM efficiency for simulations of passive optical components. BPM characteristics make it suitable for the design and simulation of photonic devices and photonic integrated circuits as waveguides, electro-optic modulators, Multi-Mode Interference (MMI) couplers, Y-splitters, optical delay lines and others. Its weakness lies in a simulation of structures with a high contrast of refractive index as well as structures with dimensions below the incident wavelength. Another shortcoming stems from its inability to incorporate optical radiation propagating primarily in any other than z direction, which might include bends and other devices [25, 26].

Finite element method

Unlike the BPM, the FEM (Finite Element Method) is most suitable for complex geometries and materials with high refractive index contrast. The basic concept of FEM consists of splitting the computational domain into discrete regions (or elements) and subsequently finding local solutions satisfying the differential equations within the boundaries of this region. Afterwards, a global solution can be obtained by assembling the individual solutions of these regions back together; therefore, the resulting field is calculated over the whole domain. This simulation method offers very precise results for a wide variety of problems; however, it offers very computationally demanding solutions in cases including a wide range of wavelengths/frequencies. In order to calculate propagation in a broad spectrum, other computational methods like finite-difference time-domain are usually favourable [27, 28].

Finite-difference time-domain

The Finite-Difference-Time-Domain (FDTD) method is most commonly used for simulations of integrated optics, mainly in circuits and structures that can cause difficulties that the BPM method cannot cope with. The result of the FDTD method is a rigorous solution to Maxwell's equations. This method can also include many more effects than other approximation methods since it is a direct solution of Maxwell's equations.

This method's most significant advantage lies in its versatility because FDTD is inherently full-vectorial without limitations on optical effects such as the direction of propagation, index contrast, or backward reflections. The FDTD method is also suitable for handling material dispersions, nonlinearities, and simulations with a wide frequency range in a single simulation run since it is based in a time domain.

The main disadvantage of this method lies in its computational demands. It requires a relatively dense grid of points at which all three(or 2 for 2D simulations) vector components of the electric and magnetic fields must be maintained. Even a simple photonic device like a directional coupler can provide quite a tough challenge for the computer using the FDTD method due to the relatively long dimensions of the coupler.

In order to keep simulation time reasonably short, a computer with terabytes of memory would be required [29].

Rigorous coupled wave analysis

The Rigorous Coupled Wave Analysis (RCWA) is a frequency-based simulation method calculating the diffraction efficiencies. It represents the electromagnetic fields as a sum over coupled waves. Each coupled wave is related to a Fourier harmonic (used to represent the periodic permittivity function of discretised spatial layers of the structure), allowing the solution of full vectorial Maxwell's equations in the Fourier domain.

It is suitable for 2D or 3D simulations of periodic structures, photonic bandgap crystals, subwavelength structures, and other grating-assisted devices. This algorithm is able to process a wide range of scattering problems on structures with horizontally periodic boundary conditions. Even arbitrarily vertical variations can be handled; however, the cover and substrate (two semi-infinite regions) must be homogenous [30].

Eigenmode expansion method

If an appropriate numerical limit is used, the EigenMode Expansion method (EME) is rigorous, fully vectorial, and omnidirectional. While being a rigorous solution to Maxwell's equations, in contrast to FDTD, it can still accurately deal with very long structures. However, the common trade-off between computational demands and precision occurs using this technique. It is most commonly used to calculate electromagnetic wave propagation in various structures, both two and three-dimensional [31].

3 Design and simulations

This chapter contains a design supported by a simulation of photonic structures and devices for sensor applications, as well as auxiliary circuits designed to turn the sensor structures into possible lab-on-chip applications.

3.1. Multi-mode waveguide-based refractive index sensor with a plasmonic layer

The first proposed sensor is a multi-mode waveguide-based plasmonic refractive index sensor with direct contact of a metal layer with a waveguiding core. In the work, two variations of such sensor were presented to showcase the proposed sensor's and material platform's versatility and provide solutions for refractive indices of all commonly used liquid analytes (RI anywhere between 1.2-1.6 [32]).

As a material platform, Si_3N_4/SiON was chosen due to its transparency for visible wavelengths range and refractive index tunability, which proves to be a key parameter in the design of this sensor type. According to the work of Čtyroký et al. [33] for this type of sensor, due to its underlying physical principle, the position and attenuation of a dip in a spectrum are highly dependent on both refractive indices of an analyte, as well as the waveguiding core. Therefore, to maintain good sensitivity with spectral dip occurring in visible wavelengths, the sensor must consist of a waveguiding core with a refractive index similar to the analyte's refractive index.

The cross-section of the proposed material platform is shown in Fig. 3.1, where a silicon wafer was chosen as a substrate for the device, on top of which the SiO_2 buffer layer with a thickness of 2–10 μm is expected to be grown by available methods like plasma enhanced chemical vapour deposition. SiON material is expected to be grown on the top of the buffer layer using the same growth method while adjusting the parameters to obtain the desired refractive index. Finally, the whole waveguide is to be passivated by a thick layer of SiO_2 to prevent the analyte's interaction with the non-sensing part of the waveguide.

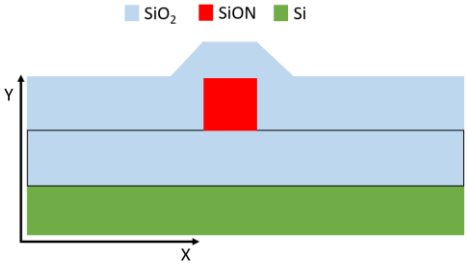

Fig. 3.1 Transversal cross-section of used material platform for waveguide.

The final structure of the sensor consisting of four distinct layers is shown in Fig. 3.2, with the SiO_2 cladding layers (n = 1.46) thick enough to optically separate the waveguiding layer from the Si substrate and environment, waveguiding layer (SiON), and a gold layer on top of core in the sensing part. Gold has been chosen as the metal layer due to its strong plasmonic resonance capabilities combined with chemical stability in various environments.

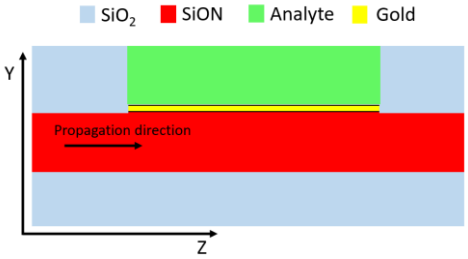

Fig. 3.2 Longitudinal cross-section of the multi-mode plasmonic waveguide sensor strip.

The optimal parameters of the sensor (e.g. waveguide's width, thickness, gold layer length and gold layer thickness) were investigated in order to provide the most suitable platform for the sensor. The sensor part with plasmonic structure was designed and simulated using the Eigenmode Expansion Method incorporated into the ModePROP module of RSoft Photonic Device Tools due to its computational simplicity synergising well with a relatively long waveguiding model as well as with its ability to solve photonic calculations, including the plasmonic effect. Consequently, two SPR sensors suitable for detection of different liquid analytes are proposed, with the only difference being

the refractive index of their respective cores, as the two optimal values of the core's RI 1.55 and 1.8 were chosen with the aim of covering all the liquid analytes with refractive indices from 1.3 to 1.6 (liquid analytes with RI of 1.2 to 1.3 are rarely used; however, if the necessity arises, sensitivity for them can still be obtained by proposed sensor structure). Their transmitted optical power spectra for different refractive index ranges are shown in Fig. 3.3.

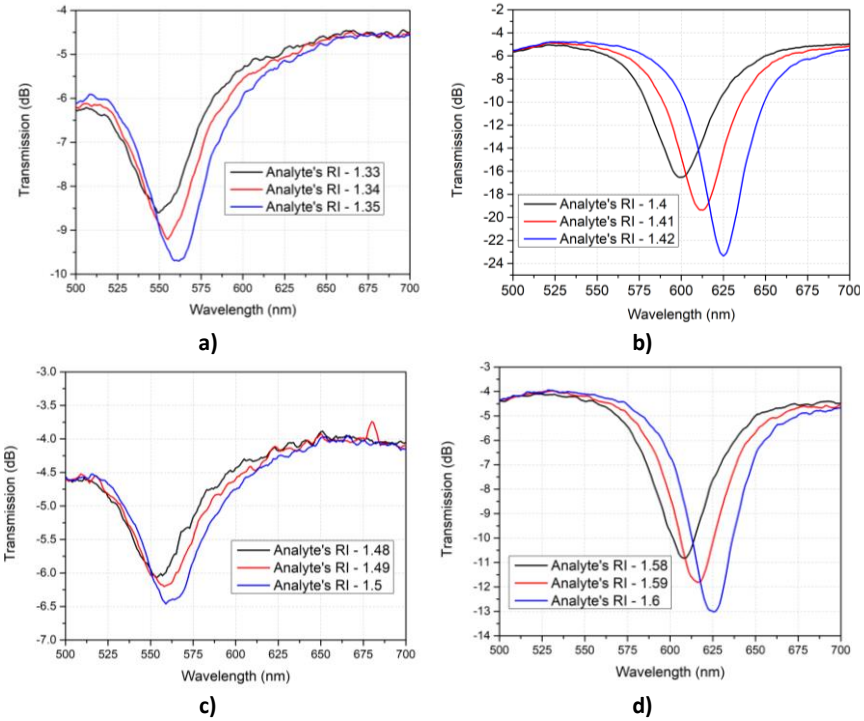

Fig. 3.3 Sensitivity of proposed sensor to different RI of analyte: a) for SiON with RI of 1.55 and lower RI of analyte; b) for SiON with RI of 1.55 and higher RI of analyte range; c) for SiON with RI of 1.8 and lower RI of analyte; d) for SiON with RI of 1.8 and higher RI of the analyte.

For better visualisation, sensitivity, and Figure of Merit (FoM), dependence on the refractive index of the analyte is shown in Fig. 3.4. It can be seen that both of these parameters are nonlinear, where with the analyte's RI approaching the refractive index of the core, the spectral shift is increasing. According to simulation results, the sensitivity of the sensor (calculated as theoretical spectral shift corresponding to a change of refractive

index of analyte by one unit) with the core's refractive index of 1.55 is approximately 500 nm/RIU (Refractive Index Unit) for a lower range while improving to more than 3000 nm/RIU for higher ranges. On the other hand, if the sensor is adjusted to be sensitive for analytes with refractive indices over 1.5 (therefore changing the core's RI to 1.8), the presented sensitivity is approximately 200 nm/RIU and 1000 nm/RIU, respectively. As mentioned before, it shows strong nonlinearity (which corresponds to increased sensitivity), while the analyte's refractive index approaches that of the waveguide's core.

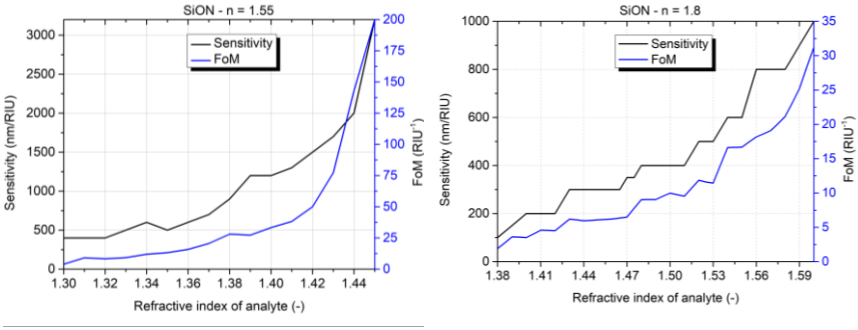

a) **b)**

Fig. 3.4 Sensitivity and Figure of Merit dependence on the analyte's refractive index: a) for waveguide sensor with a refractive index of core n = 1.55; b) for waveguide sensor with a refractive index of core n = 1.8.

The result shows that the two proposed sensors are able to cover a range of analytes with a refractive index from 1.3 to 1.6. The first sensor with a refractive index of core 1.55 offers sensitivity for RI from 1.3 to 1.44. The second proposed sensor with a core RI of 1.8 covers the rest of the possible liquid analytes with a sensitivity from 1.38 to 1.6. As shown in Fig. 3.4, the potential achievable sensitivity of the sensor is more than 3000 nm/RIU and the Figure of Merit obtained from simulations was more than 200 RIU^{-1}. The proposed sensor's potential sensitivity is more than four times higher than Bragg gratings [34], silicon [35], and MIM structures [36] while also boasting comparable or even higher FoM. Higher sensitivity was usually achieved only using more complex structures like ring resonators [36] or by introducing multi-stack layers into the design [21], which might also be a possible future area of research for the sensor proposed in this paper. In addition, its

multi-mode character offers the possibility of a relatively long sensing structure with a comparably low attenuation to provide ease of use in a non-lab environment.

Finally, spectra presenting the sensitivity of the sensor show strong nonlinearity, which only further proves that sensitivity increases more rapidly while approaching the waveguide's refractive index, thus, promoting the adjustability of the SION material platform to balance the sensor's sensitivity and loss by adjusting the RI parameter of the core. With a refractive index of the SiON material platform ranging from values of SiO_2 (1.456) to Si_3N_4 (2.0) for visible wavelengths, it can be said that the platform, as well as the design, should be capable of sensing not only any commonly used liquid analyte but even solids in solutions or common water pollutants.

3.2. Single-mode waveguide-based refractive index sensor with a separated plasmonic layer

The second proposed refractive index sensor is a waveguide-based plasmonic sensor with of metal layer separated from the waveguiding core by a passivation layer. Si_3N_4/SiON was chosen as a material platform for similar reasons as in the previous chapter, e.g., visible range transparency, refractive index adjustability, low losses, CMOS compatibility etc. The cross-section along the propagation direction of the sensor is shown in Fig. 3.5. The change from a multi-mode to a single-mode sensing platform offers easier integrability and lower demands on fabrication resources while maintaining similar sensitivity. It is most suitable for applications where easier integrability into complex circuits is more important than coupling and total transmitted power.

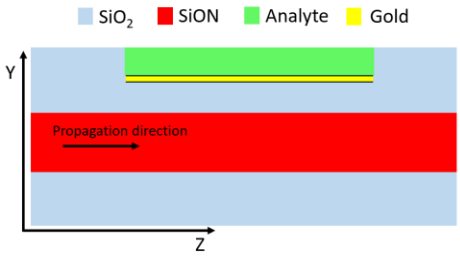

Fig. 3.5 2D geometry of the proposed single-mode plasmonic waveguide sensor strip.

In the case of previously proposed sensors, where the metal layer is in direct contact with the waveguiding core, the length of the metal layer is fairly limited due to the underlying physical principle. If the length of the sensor part is too short, the plasmonic dip is not pronounced enough in the spectrum, and the sensitivity diminishes. On the other hand, if the plasmonic layer is too long, the attenuation becomes too strong, and the propagation through the waveguide is completely suppressed. This design offers an alternative solution to this problem, where instead of depending on the number of propagating modes, the transmission and spectral dip pronunciation is determined by the combination of the thickness of the separation layer and the sensing layer length. EME was used for the simulation due to the same reasons as in the previous case. After the sensor parameters were determined and the design was finished, spectral characteristics using various analytes were investigated. The results are shown in Fig. 3.6, where a clear spectral dip shift can be seen with the analyte's refractive index change. However, the figure shows two sets of spectral dips caused by the plasmonic effect. First, between 550-650 nm offers higher sensitivity, with the trade-off being rapidly increasing attenuation (therefore offering only a small range of suitable analytes). And the second, between 650-750 nm, which was targeted during optimisation due to the versatility requirements of the sensor.

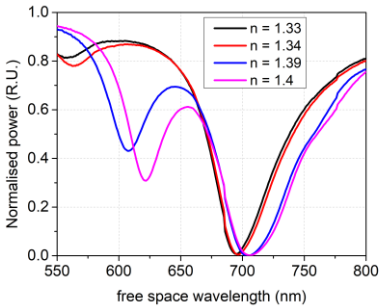

Fig. 3.6 Spectral characteristics of the single-mode waveguide-based sensor for various refractive indices of water-based analytes.

Subsequently, the sensor focused on shorter-wavelength spectral dip was designed using the same optimisation process. Due to the low change in attenuation with

the change in the analyte's refractive index, the sensor focusing on the dip occurring at~ 700 nm is able to provide reliable sensitivity for a wide range of analytes. It can cover the range of most commonly used analytes in a lab environment (1.33-1.45). On the other hand, for the dip occurring at~ 600 nm, there is a substantial increase in attenuation with the analyte's refractive index change, which prevents it from being used in the same range.

Therefore, two separate sensor configurations need to be used to sense analytes in the above-mentioned range. These configurations might be obtained by the adjustment of separation layer thickness, therefore removing the necessity for further optimisation or separate photolithography mask. As in the case of the previously proposed multi-mode waveguide-based sensor, the sensitivity and Figure of Merit are plotted to improve the visualisation of sensors' performance and suitability for application. These parameters are shown in Fig. 3.7, where both configurations for dip around 700 nm and 600 nm of wavelength are taken into consideration. The line which represents the dip occurring in shorter wavelengths is split into two parts to represent two different thicknesses of separation layer aimed at sensing two different parts of the analyte's refractive index range (1.33-1.45). The line representing the dip in the longer wavelength range is, however, continuous due to the possibility of its use in the whole range.

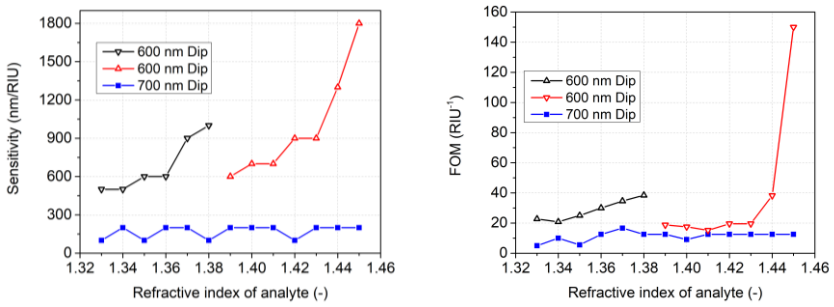

a) **b)**

Fig. 3.7 Dependence on the analyte's refractive index for: a) sensitivity and b) Figure of Merit.

The sensor with a gold layer length of 100 µm, thickness of 50 nm and 700 µm wide gap shows a sensitivity of~200 nm/RIU (refractive index unit), and the sensor with a gold

layer 700 µm long and 1 µm wide gap shows a sensitivity of 250-300 nm/RIU. From the results shown in Fig. 3.7, it can be seen that by optimisation aimed at the plasmonic dip occurring in shorter wavelengths, the sensitivity of the sensor might be increased from 200 nm/RIU to more than 1800 nm/RIU while limiting its usability to shorter range of refractive indices. At the same time, the FoM proved to reach more than 150 RIU^{-1}. This proves the match in terms of sensitivity and even overcomes in the Figure of Merit, commonly used waveguide and SPR-based refractive index sensors [36, 37].

Therefore, results show that depending on the desired central wavelength, the designed single-mode-based SPR sensor might offer better solutions for applications where total transmitted power and coupling are not of particular concern. Furthermore, this sensor was optimised for the most commonly used liquid analytes; however, thanks to the SiON material platform, the refractive index of the core might be increased to offer sensitivity in higher ranges, offering the possibility of label-free sensing of solids in solutions or any common pollutants.

3.3. Design of the first iteration of the auxiliary circuit

Two iterations of auxiliary circuit are presented in this work. The first one is designed for initial measurements and confirmation of the multi-mode waveguide-based sensor's sensing capabilities and sensitivity. Therefore, the whole circuit is built on an 8 µm waveguide platform, with structures like coupling/decoupling grating (even though being far from optimal from the coupling efficiency point of view for the SiON material platform) being used due to their characterisation simplicity and compatibility with our measuring and coupling equipment. The circuit (shown in Fig. 3.9) consists of coupling and decoupling grating situated on a 200×200 μm^2 pad, considered big enough to encompass the whole radiated field from in-coupling multi-mode fibre. Following the pad, two tapers are situated on the input/output part of the multi-mode waveguide, which has a metal sensing strip in the middle of the linear platform. Fig. 3.8 3D model of the first circuit design with a passivated structure. All the passive components of the auxiliary circuits in this work were designed using BPM and FEM methods, with the only exception being the coupling grating where FDTD was used due to the complexity of the simulation model.

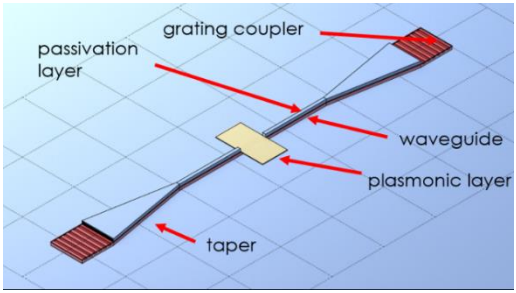

Fig. 3.9 3D model of first circuit design with passivated structure

For the needs of the photolithographic process, a mask supporting the fabrication of the above-mentioned circuit was designed. It consisted of nine distinct patterns designated for a sample size of 16×16 mm^2.

Fig. 3.10 shows the whole design with a photolithography mask. It contains the whole proposed circuit designed for the width of waveguides of 2, 4, 6, and 8 µm., coupling grating for the 8 µm wide waveguide sensor, plasmonic layer pattern and grating protection pattern for deep etching of the rest of the waveguide.

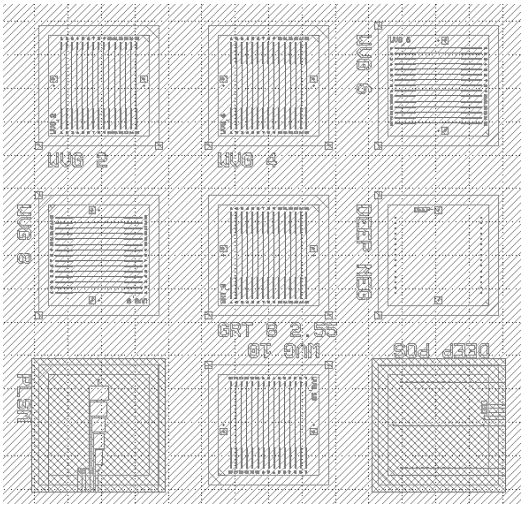

Fig. 3.10 Layout of whole photolithography mask designed for the fabrication of first circuit supporting waveguide-base plasmonic sensor.

3.4. Design of the second iteration of the auxiliary circuit

The second iteration of an auxiliary circuit for the waveguide-based plasmonic sensors is based on a single-mode waveguide platform, with the multi-modal part only being in the sensor area. This change allows much easier utilisation of photonic structures such as splitters, bends, and others, helping with easier and more precise sensor optical output characterisation. The circuit coupling is proposed via the taper method, which shows to be the most appropriate for the chosen material platform. This coupling structure is followed by a 90 ° bend, which ensures the separation of input fibre-mode (especially in the case of thick multi-mode fibres and output modal field of the circuit). Due to the spectral dependence of many structures in the circuit, as well sensor itself, the reference branch is created by either multi-mode interference (MMI) splitter or directional coupler in order to verify the actual spectral output of the sensor, removing the potential bias created by the rest of the circuit. Lastly, another bend is positioned after the splitter to direct the light on the opposite side of the substrate to allow easier fitting of other circuit patterns onto the same substrate field. After the bend and short linear single-mode part, either sensor design is implemented into both branches, with one branch being covered by a gold layer in a later fabrication process. One of the circuit iterations is shown in Fig. 3.11, where there is no single to multi-modal platform adaptation, and S-bend is used instead of a 90 ° bend.

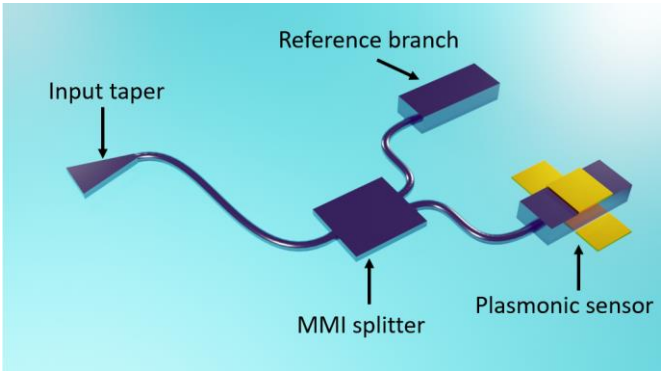

Fig. 3.11 One of the single-mode-based auxiliary circuit adaptations.

A second photolithography mask needed to be designed to fabricate the aforementioned photonic devices based on single-mode waveguides. The whole design can be seen in Fig. 3.12. As in the previous case, the mask consists of 9 distinctive patterns. However, contrary to the previous case, the sample size increased from 16×16 mm^2 to 20×20 mm^2. This change was allowed by adjustment in the fabrication process, where instead of using only one segment of a pre-cut substrate, the whole photolithography mask is used, and all the patterns are etched simultaneously. This allows easier sample handling during measurements and better contact during mask exposition.

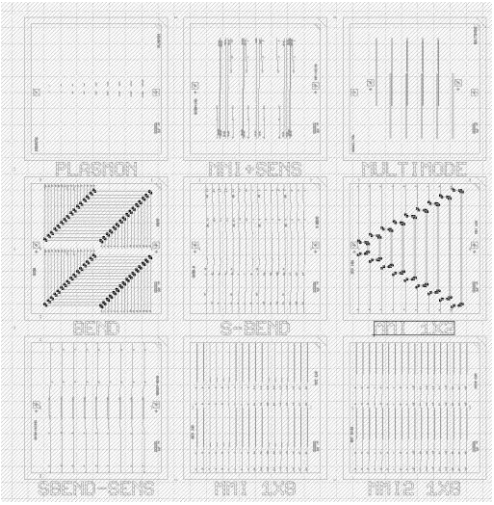

Fig. 3.12 Layout of the whole photolithography mask.

The respective patterns are aimed at the MMI, 90 ° bend, S-bend, and plasmonic sensor characterisation, as well as at plasmonic layer pattern creation.

3.5. Near-field probes based on nanocone and nanopyramid structures

In addition to previously proposed sensors and auxiliary circuits, IP-Dip-based sensor structures, prepared and measured in collaboration with the Technical University of Žilina, were designed and optimised.

The subwavelength-confined and enhanced optical fields push the limits in optical characterisation, manipulation, and processing on the nanometre scale. However, characterisation on the nanometre scale still poses a challenge. To help overcome this issue, near-field probes positioned on the tip of a fibre are often used. They usually consist of dielectric structures coated by a thin metal layer to take advantage of the resonant properties of conductive nanosystems due to the surface plasmon polaritons arising at the metal-dielectric interface [38].

In the work, two basic types of metal-dielectric near-field probe structures are presented. Nanocones 5 and 6 μm high with a circular base with 10 μm diameter, and nanopyramids with square base with a width of 10 μm and the same two heights. The dielectric part consists of IP-Dip polymer (n = 1.52 at 780 nm unexposed) and the thin (10 nm) metal gold layer. The structures were designed in collaboration with the Department of Physics of the Faculty of Electrical Engineering and Information Technology University of Žilina and consequently fabricated by this department using Nanoscribe Photonic Professional GT by Nanoscribe GmbH. Nanoprobes were investigated using both the FDTD and RCWA simulation methods; however, in order to obtain the most precise field intensity and distribution in the close vicinity of the probe, the FDTD method was chosen as optimal. Resulting near fields at a distance of 50 nm (Fig. 2.13) from the probes' tips show that more focused radiation is extracted from the tip. The circular symmetry of nanocones causes a halo effect that is more blurred with an increasing wavelength of radiation. On the other hand, the edges of nanopyramids result in a diffraction effect, which generally reduces the focus of radiation above the tip of the NP, rendering them least ideal.

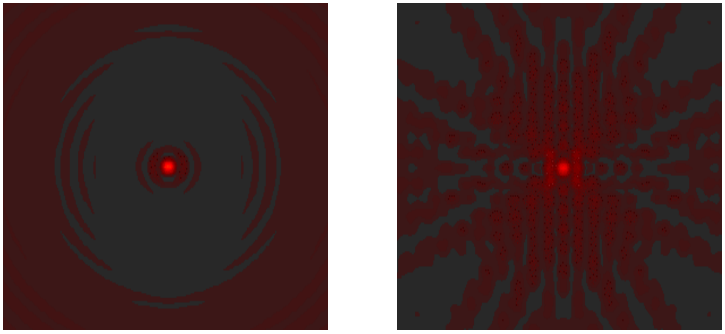

a) **b)**

Fig. 3.13 Near-field intensity map simulated at an area of 8x8 µm, 50 nm above the a) nanocone and b) nanopyramid.

Consequently, profiles of nanocones and nanopyramids from the point of near-field intensity and the resolution calculated as FWHM are summarised in Tab. 3.1 . During the investigation phase, the wavelength of 420 nm proved to offer the best resolution among the tested ones, therefore, was used for further optimisation. The best FWHM was achieved for 6 µm nanocone (151 nm), and the best signal enhancement was achieved for 5 µm high nanocone.

Tab. 3.1: Comparison of important parameters of nanocones and nanopyramids.

	Height (µm)	Intensity maximum (A.U.)	FWHM (nm)
	5	**5.2**	195
	6	1.8	**151**
	5	4.0	233
	6	4.2	177

The results are promising for designing an ideal structure that would be subsequently implemented on the front of the optical fibre - creating a Near-field Scanning Optical Microscope (NSOM) probe with an increased optical field at the tip and with the best possible resolution.

4 Fabrication

In general, the fabrication process of most silicon-based waveguides consists of three distinct stages: thin film deposition, photolithography, and etching. The same can be said about the SiON circuit preparation technological process, only with minor changes, namely the necessity of annealing. After the core layer is fabricated, a cladding layer is deposited on top if specified. The fabrication process is not the main focus of the work; therefore, this chapter is included only to provide the complete picture of the sensor creation process. The deposition of dielectric layers

The fabrication process of the SiON photonic structures consists of the following steps:

1. Deposition of SiO_x passivation (buffer) film
2. Deposition of the SiON optical waveguide core film
3. Annealing of the SiON layer
4. Metal layer deposition
5. Photolithography
6. Wet etching of the metal layer
7. Plasma etching of the SiON film
8. Removal of remaining photoresist and metal layer
9. Deposition of the SiO_x cladding film

All the fabrication was done by available technologies at IEP FEI STU. All the dielectric layers were deposited by Plasma Enhanced Chemical Vapour Deposition (PECVD) using Plasmalab 80+ from Oxford Instruments. Metal layers intended as a photolithography mask and a potential plasmonic layer were deposited by Physical Vapour Deposition (PVD) using PRO Line PVD 75 from Kurt J. Lesker Company. Additionally, the photolithography for direct pattern transfer was done using a mask aligner and exposition chamber (MA/BA6 from SUSS MicroTec SE. And finally, the etching of dielectric layers was done by inductively coupled plasma reactive ion etching (ICP-RIE) in Plasmalab 100 from Oxford Instruments.

5 Characterisation

The last part of the work deals with topographical and spectral characterisation of proposed structures. As the initial structure for fabrication and consequently coupling optimisation, the waveguides with 8×8 μm^2 cross-section profile were fabricated. The pattern with embedded coupling grating was chosen to offer the possibility of out-of-plane coupling via grating while still allowing cutting samples and polishing the edges for in-plane coupling.

5.1. Coupling grating characterisation

The etch depth, as well as grating period and fill factor, were investigated using High Dynamic Range (HDR) enhanced confocal microscopy, Atomic Force Microscopy (AFM), and Scanning Electron Microscopy (SEM). Exemplary results are shown in Fig 4.1.

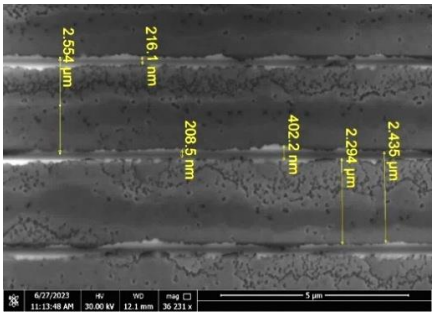

a)

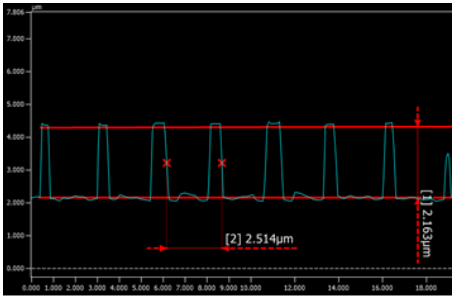

b)

Fig. 5.1 a) Cross-sectional profile of coupling grating acquired by confocal microscopy. b) SEM image of coupling grating.

All the SEM images were obtained in collaboration with the Slovak Academy of Sciences. It is transparent that even though the period stayed consistent with the mask pattern (2.55 μm), the fill factor and etch depth do not correspond to the desired values (50% for fill factor and 2.4 μm for etch depth). The results show that the high refractive index part of the grating has varying thicknesses of ~200-500 nm, corresponding to only a 13-20 % fill factor.

Concerning the slightly lower etch depth, longer etching in RIE should be a sufficient solution. On the other hand, the alteration in fill factor might be caused by several factors, where the two most prominent are light diffraction on the mask during the exposure process and the possible unsuitability of wet etching as a process of choice for pattern creation using a metal mask for micrometric periodic structures. If the coupling grating is to be used in future applications, the fabrication process will need to be revised, preferably incorporating electron beam lithography into the grating structure creation.

After topographical characterisation was concluded, the optical measurements were carried out to find the most suitable coupling angle in and out of the grating. The imprecision in creating the coupling grating also caused a significant decrease in coupling efficiency, rendering the grating coupler for simultaneous in-coupling and out-coupling near impossible. Only two approaches were therefore used in the work. Hybrid one, where one side is cut somewhere in the tapering region and polished for in-plane coupling, while out-coupling was done by grating, and the second one, where both of the sides are cut edges, and both fibres are positioned opposite to these polished edges of the sample. The first configuration allowed for angle measurements of grating characteristics to obtain the ideal angle under which the coupling fibre should be positioned.

The average of the results can be seen in Fig. 4.2, correlated with simulation results. As can be seen from the topography measurements, the fill factor itself varies alongside grating. Therefore, finding a model with a constant fill factor that would fit the measurement results was impossible. Consequently, the curve representing simulation results in Fig. 4.2 is the average of results for fill factors of 10-20 % with the step of 1 %. Two distinct local maxima occur in experimentally obtained curves at roughly 20 °

and 60 °, calculated as a distance from the axis perpendicular to the grating. The comparison with simulation results confirms the resulting physical dimensions of the grating. The simulation was carried out using all the supported TM modes of the multi-mode waveguide as an input field.

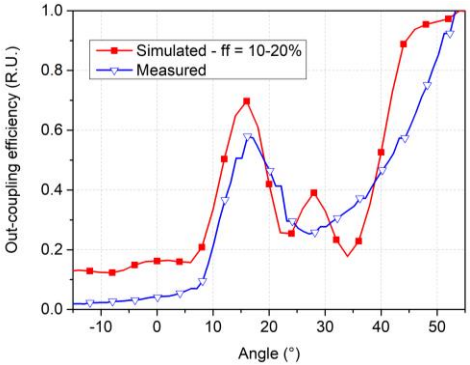

Fig. 5.2 Correlation between angular measurement and simulation of out-coupling radiation from grating coupler.

5.2. Sensor characterisation

Since the optimisation of passivation and consequent "opening" of a window on top of the waveguide to allow direct deposition of a gold layer onto the was not fully optimised during the time of finishing this thesis, proper measurement of sensitivity posed a significant challenge. To limit the possibility of the analyte's interaction with the non-sensing part of the waveguide, therefore influencing the measurement, only the small drops applied by a micro-pipette were used during the measurements.

The resulting spectra can be seen in Fig. 5.3, where the influence of the white LED source is prevalent in all the measurements (as shown in Fig. 5.3 a)). Therefore, to only obtain the spectral influence of the analyte, the transmission through the waveguide sensor without the analyte was subtracted from the result with the analyte and compared to the simulation (Fig. 5.3 b)). The simulation was likewise adjusted to reflect the droplet size and length of the plasmonic layer. There can be seen a clear correlation between these two curves and their respective dips, and therefore it can be concluded that the sensor is sensitive to analytes with a refractive index of around 1.33. Even though

the initial measurements proved to be optimistic, further investigation using different analytes with various refractive indices is necessary to fully assess the sensitivity and usability of the proposed sensor. This further investigation, however, should only occur after optimisation of passivation and consequent "window" opening to ensure reliable and repeatable results.

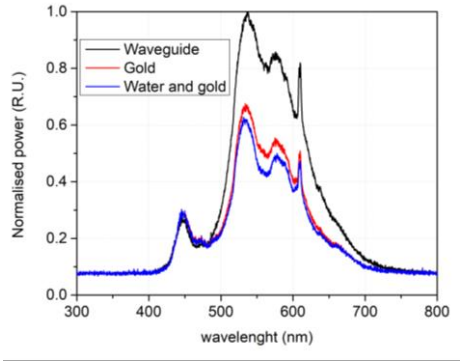

a)

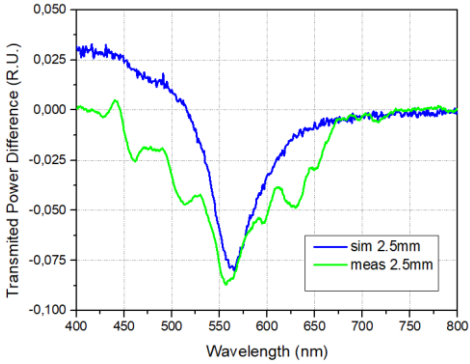

b)

Fig. 5.3 a) Transmission through the waveguide without a gold layer, with a gold layer and with a gold layer and analyte applied. b) The spectral response of multi-mode waveguide with gold layer after analyte application.

Summary

The thesis consisted of four distinct parts. In the first part, waveguides, their material platforms and coupling possibilities were studied and briefly described to provide a basis for further design and fabrication of various photonic devices. Namely, Silicon Oxynitride was chosen as a material due to its unique properties like visible wavelength transparency, refractive index adjustability and CMOS compatibility. In addition, it provided state-of-the-art for waveguide-based plasmonic sensors, which are this work's main topic.

The second part provided a description of available simulation methods, the choice of which is a vital step in the creation of an appropriate and precise simulation model and the simulation design itself. Consequently, the simulation design of two distinctive waveguide-based SiON-plasmonic sensors was presented. The first, based on a multi-mode waveguide, can provide sensitivity for a considerable variety of analytes, taking advantage of the aforementioned refractive index adjustability of the SiON platform. Its optimal thickness, length of sensing strip, as well as plasmonic layer thickness were investigated, with results showing that the potential achievable sensitivity of the sensor is more than 3000 nm/RIU, while the Figure of Merit obtained from simulations was more than 200 RIU^{-1}. This value matches commonly used waveguide and SPR-based refractive index sensors in terms of sensitivity and even overcomes them in the Figure of Merit [36, 37]. The second sensor based on a single-mode waveguide was consequently investigated for the same parameters. The results show a trade-off in potential sensitivity for its easier integrability to another circuit. After optimisation, the potential sensitivity of the sensor obtained rose to 1800 nm/RIU with FoM 150 $RIU^{-1,}$ which, even though proving to be lower than in the case of a multi-mode-based sensor, is able to be a match for the commonly used sensors in literature [36, 37]. For both sensors, auxiliary circuits were designed, consisting of various coupling possibilities, bends, and splitters providing easy measurement and characterisation. Consequently, two photolithography masks were created to allow the fabrication and characterisation of all proposed devices and structures. Furthermore, in collaboration with the University of Žilina, IP-Dip-based NSOM probes coated by a thin layer of gold were investigated, while their fabrication and

characterisation were done by the University of Žilina research team. The results of the investigation were optimal parameters for NSOM probe fabrication.

The third part of the work presents fabrication methods and devices available at IEP FEI STU alongside the technological fabrication process of proposed structures. This chapter is, however, relatively brief due to its content not being the focus of the proposed work, while the chapter's only aim is to provide a complete picture to the reader about all steps of the sensor's creation, from design through fabrication to characterisation.

Therefore, the last part of the work focused on the analysis of topological as well as optical characterisation of some of the proposed structures. Firstly, the topological characterisation of the multi-mode waveguide-based SPR sensor and its coupling grating was analysed using several available methods. The results showed mainly two imperfections in the fabrication process. The first one is insufficient etch depth of the grating and waveguide, which is easily adjustable by increased etching time. However, the results also showed significant under-etching of proposed structures. It was most probably caused by an under-etching of the metal mask during direct mask pattern transfer using the wet etching method of the metal layer. While it does not decrease the functionality of the proposed sensor itself, it significantly decreases the efficiency of the proposed grating coupler, shifting the fill factor from 50 % to less than 20 %. Both simulation and characterisation results then showed the efficiency to be too low for use in the proposed application. Therefore, the sensor was optically characterised by using the direct coupling method. Due to the passivation process being in the optimisation stage during this thesis's writing, all of the sensor structures were not passivated, bringing a risk of analyte interacting with the waveguide even outside of the sensing area. Therefore, only a small amount of liquid with suitable viscosity could have been used to ensure it remained in the sensing area. This constraint, however, affects the repeatability of the sensing due to the different viscosities of different analytes affecting the droplet diameter and interaction length with the sensor. Thus, only its basic functionality was tested using demineralised water and observing the formation of the characteristic spectral dip. This result shows promise towards future optimisation and usability of this sensor.

Main results of the thesis

1. New knowledge was obtained to identify the most suitable methods for simulation and optimisation of specific photonic structures for sensor applications.

2. Two iterations of an auxiliary circuit for photonic sensor characterisation and integration into PIC were designed and optimised, while photolithography masks were created for consequent fabrication and characterisation.

3. Multi-mode waveguide-based SPR sensor was designed and optimised. It is sensitive to an extensive range of analytes while maintaining outstanding sensitivity, transmission efficiency and Figure of Merit.

4. Single-mode waveguide-based SPR sensor was designed and optimised. It covers a wide range of liquid analytes while being relatively robust. It brings a relatively big sensing area compared to commonly used waveguide-based sensors. Lower sensitivity and transmission efficiency in comparison with multi-mode sensors is offset by easier integrability into PIC due to its single-mode nature.

5. IP-Dip-based NSOM probe was designed and investigated. The results were correlated with measurements showing promise towards tip-of-fibre applications.

6. Multi-mode waveguide-based SPR sensor and its auxiliary circuit were characterised by topographical and optical methods. The results provided feedback to the fabrication process and proved the sensing capabilities of the proposed design.

Resumé

Jedným z najbežnejších využití fotonických prvkov sú senzorické aplikácie, ktoré sú schopné na báze zmien vlastností žiarenia detegovať rôzne parametre ako zloženie materiálu, index lomu, hrúbka, ale aj mnoho ďalších. Veľa pozornosti v tomto odvetví priťahuje najmä využitie povrchovej plazmonickej rezonancie (SPR), ktorá bola predmetom veľkého množstva teoretických, ako aj praktických štúdii počas posledných 20 rokov. Jednou z jej najdôležitejších vlastností sú schopnosť poskytnúť v reálnom čase meranie rôznych fyzikálnych, chemických a biologických kvantít a zosilnenie spektrálnej odozvy v už existujúcej fotonickej aplikácii. Využitie povrchových plazmónov je základom veľkého množstva senzorických aplikácii ako napríklad Kretschmann-ove a Otto-ve konfigurácie, vláknové senzory, ale aj vlnovodné senzory, ktoré ponúkajú možnosť integrácie do zložitejších fotonických obvodov. Práve návrh, výroba a meranie vlnovodných senzorov skombinované s plazmonickými vrstvami boli hlavným predmetom tejto dizertačnej práce.

Práca sa v úvodnej časti zaoberá práve princípom fungovania rôznych typov vlnovodov, používaným materiálovým platformám a princípom naviazania optického žiarenia z vlákien do vlnovodov. Tieto poznatky následne tvoria základ návrhu všetkých fotonických prvkov v práci. Pre účely tejto práce bol zvolený materiál SiON (oxynitrid kremíka), ktorý vďaka svojej CMOS kompatibilite a nastaviteľnému indexu lomu ponúka cenovo dostupné a široko-uplatniteľné riešenie pre rôznorodé fotonické aplikácie. Ďalšou z jeho výhod je jeho priehľadnosť vo viditeľnom spektre optického žiarenia, ktoré je najvyužívanejšie pri bio-senzoroch. Je to platforma s relatívne nízkymi hodnotami kontrastu indexov lomu, preto sú pre ňu charakteristické pomerne nízke materiálové straty, aj keď za cenu zložitejšieho optického naviazania žiarenia.

Následne sú v práci popísané základné fyzikálne princípy budenia a využitia povrchových plazmónov, akými je napríklad ramanovská spektroskopia, alebo vyššie spomenuté vlnovodné senzory využívajúce povrchovú plazmonickú rezonanciu. Pre tento typ senzorov je popísaný stručný prehľad súčasného stavu problematiky, ktorý tvorí základ návrhu senzorov v tejto práci.

Pre doplnenie všetkých teoretických poznatkov potrebných k vytvoreniu najvhodnejších simulačných modelov sú predstavené simulačné metódy použité v tejto práci. Pre vykonávanie simulácií bol v práci používaný softvérový nástroj RSoft Component Design Suite, ktorý integruje viaceré numerické metódy využiteľné pre daný typ prvku či aplikácie.

V rámci časti práce venujúcej sa numerickým simuláciám boli navrhnuté 3 rôzne typy senzorických štruktúr. Prvou bola multi-módová vlnovodná senzorická štruktúra využívajúca SPR. Hlavným cieľom tohto návrhu bolo poskytnúť integrovateľnú senzorickú štruktúrú, vhodnú pre veľký rozsah indexov lomov analytov, ktorá bude mať citlivosť porovnateľnú s jedno-módovými vlnovodnými senzormi, avšak ponúkne širšiu senzorickú spektrálnu oblasť a potencionálne vyššie prenosové úrovne. Bola preskúmaná jej optimálna hrúbka, dĺžka senzorickej oblasti a hrúbka kovovej-plazmonickej vrstvy, pričom výsledky ukázali, že potenciálne dosiahnuteľná citlivosť senzorickej štruktúry je viac ako 3000 nm/RIU, zatiaľ čo hodnota FoM (z anglického Figure of Merit) získaná zo simulácií bola viac ako 200 RIU^{-1}. Táto hodnota sa zhoduje s bežne používanými senzormi indexu lomu na báze vlnovodu a SPR z hľadiska citlivosti a dokonca ich prekonáva v hodnote FoM [36, 37]. Druhá senzorická štruktúra založená na jedno-módovom vlnovode využívajúca SPR bola následne preskúmaná pre rovnaké parametre. Avšak narozdiel od predošlého prípadu, kde bola kovová vrstva v priamom kontakte s vlnovodným jadrom, bola v tomto prípade kovová vrstva oddelená od vlnovodného jadra precízne zvolenou hrúbkou pasivačnej vrstvy. Táto zmena v konfigurácii umožňuje výrazné predĺženie senzorickej časti vlnovodu. V tejto práci navrhnutá úprava dovoľuje dĺžku senzorickej časť upraviť v závislosti od špecifikácií konkrétnej aplikácie, v rozsahu od niekoľkých mikrometrov až po viac ako jeden milimeter. Výsledky simulácií ukazujú, že jej jednoduchšia integrovateľnosť v porovnaní s multi-módovou vlnovodnou štruktúrou je vyvážená relatívne nižšou citlivosťou. Po optimalizácii sa potenciálna citlivosť senzora zvýšila na 1800 nm/RIU s FoM 150 RIU^{-1}, čo aj keď sa ukázalo byť nižšie ako v prípade senzora založeného na multi-módovom vlnovode, sa dokáže sa vyrovnať bežne používaným senzorom v literatúre [36, 37].

Pre oba senzory boli navrhnuté pomocné obvody pozostávajúce z naväzovacích štruktúr, ohybov a multi-módových interferenčných deličov umožňujúcich jednoduchšie meranie a charakterizáciu daných senzorov. Boli vytvorené dve iterácie pomocného obvodu. Prvá iterácia bola zameraná len na multi-módový vlnovodný SPR senzor, kde pre naviazanie optického žiarenia z vlákna do vlnovodu bola navrhnutá naväzovacia mriežka s presne určenými parametrami. Druhá iterácia bola vytvorená s ohľadom na použiteľnosť pre oba vlnovodné SPR senzory, kde naväzovanie z vlákna do vlnovodu bude vykonávané skrz leštenú hranu vzorky. Následne boli vytvorené dve fotolitografické masky umožňujúce výrobu a charakterizáciu všetkých navrhnutých zariadení a štruktúr.

V spolupráci so Žilinskou Univerzitou boli taktiež navrhnuté a optimalizované sondy NSOM (z anglického near-field scanning microscopy) pre aplikáciu na báze polyméru IP-Dip pokrytého tenkou vrstvou zlata, pričom ich výroba a charakterizácia bola vykonaná výskumným tímom na spomenutej partnerskej inštitúcii. Výsledkom vyšetrovania boli optimálne parametre pre výrobu týchto sond.

Tretia časť práce predstavuje metódy a zariadenia dostupné na ÚEF FEI spolu s technologickým procesom výroby navrhnutých štruktúr. Každý krok je popísaný aj s jeho možnými výhodami a nevýhodami. Táto kapitola si kladie za cieľ poskytnúť čitateľovi úplný obraz o všetkých krokoch výroby senzorických štruktúr, od návrhu cez výrobu až po charakterizáciu.

Posledná časť práce sa zameriava na analýzu topologickej aj optickej charakterizácie niektorých navrhnutých štruktúr. Ako prvá bola popísaná analýza topologickej charakterizácia multimódového vlnovodného SPR senzora a jeho naväzovacej mriežky pomocou niekoľkých dostupných metód. Výsledky ukázali dve nedokonalosti vo výrobnom procese. Prvou je nedostatočná hĺbka leptania mriežky a vlnovodu, ktorá sa ľahko upraví zvýšením času leptania. Výsledky tiež ukázali nadmerné vyleptanie, ktorého výsledkom boli menšie rozmery výslednej štruktúry. Nadmerné vyleptanie bolo pravdepodobne spôsobené podleptaním kovovej masky počas priameho prenosu vzoru pri mokrej metódy leptania kovovej vrstvy. Druhou možnou príčinou mohla byť difrakcia, ktorá vznikla na samotnej fotolitografickej maske mriežky. Aj keď to nezníži funkčnosť navrhovaného senzora, výrazne to zníži účinnosť navrhovanej naväzovacej mriežky, keďže faktor plnenia

je posunutý z navrhovaných 50 % na menej ako 20 %. Na základe topografických meraní bol simulačný model mriežky upravený a jej nové charakteristiky zistené. Simulačné aj charakterizačné výsledky potom ukázali, že účinnosť je príliš nízka na použitie v navrhovanej aplikácii. Preto bol senzor opticky charakterizovaný aj pomocou metódy priameho naviazania cez leštenú hranu vzorky, kde bola mriežka z oboch strán senzoru odstránená. Pripravené senzorické štruktúry boli nezapasivované, čo prináša riziko interakcie analytu s vlnovodom aj mimo oblasti snímania. Z tohto dôvodu bolo možné použiť iba malé množstvo kvapaliny s vhodnou viskozitou, aby sa zabezpečilo, že analyt ostane len v senzorickej oblasti. Toto obmedzenie však ovplyvňuje reprodukovateľnosť a porovnateľnosť meraní, keďže rozdielne viskozity analytov ovplyvňujú priemer kvapky a dĺžku interakcie so senzorom. Preto bola testovaná iba jeho základná funkcia, kde pomocou demineralizovanej vody bol sledovaný výskyt charakteristického spektrálneho prepadu. Výsledné namerané spektrum ukazuje prepad intenzity vo viditelnej oblasti žiarenia, čo potvrdzuje citlivosť senzoru na tekutiny s indexom lomu $n = 1.33$. Následné porovnanie so simulačnými výsledkami naznačuje potencionálnu použiteľnosť senzora v budúcich aplikáciách.

References

1. CHEN, Zhigang and SEGEV, Mordechai. Highlighting photonics: looking into the next decade. *eLight*. 8 June 2021. Vol. 1, no. 1, p. 2. DOI 10.1186/s43593-021-00002-y.

2. THYLÉN, Lars and WOSINSKI, Lech. Integrated photonics in the 21st century. *Photonics Research*. 1 April 2014. Vol. 2, no. 2, p. 75–81. DOI 10.1364/PRJ.2.000075.

3. SHASTRI, Bhavin J. et al. Photonics for artificial intelligence and neuromorphic computing. *Nature Photonics*. February 2021. Vol. 15, no. 2, p. 102–114. DOI 10.1038/s41566-020-00754-y.

4. PRABOWO, Briliant Adhi, PURWIDYANTRI, Agnes and LIU, Kou-Chen. Surface Plasmon Resonance Optical Sensor: A Review on Light Source Technology. *Biosensors*. September 2018. Vol. 8, no. 3, p. 80. DOI 10.3390/bios8030080.

5. YESUDASU, Vasimalla, PRADHAN, Himansu Shekhar and PANDYA, Rahul Jasvanthbhai. Recent progress in surface plasmon resonance based sensors: A comprehensive review. *Heliyon*. March 2021. Vol. 7, no. 3, p. e06321. DOI 10.1016/j.heliyon.2021.e06321.

6. WANG, Jiawei et al. Silicon-Based Integrated Label-Free Optofluidic Biosensors: Latest Advances and Roadmap. *Advanced Materials Technologies*. 2020. Vol. 5, no. 6, p. 1901138. DOI 10.1002/admt.201901138.

7. CHEN, Yong and MING, Hai. Review of surface plasmon resonance and localised surface plasmon resonance sensor. *Photonic Sensors*. March 2012. Vol. 2, no. 1, p. 37–49. DOI 10.1007/s13320-011-0051-2.

8. ZHU, Jun and LI, Na. Novel high sensitivity SPR sensor based on surface plasmon resonance technology and IMI waveguide structure. *Results in Physics*. June 2020. Vol. 17, p. 103049. DOI 10.1016/j.rinp.2020.103049.

9. SHIBAYAMA, Jun et al. Kretschmann- and Otto-type surface plasmon resonance waveguide sensors in the terahertz regime. *Microwave and Optical Technology Letters*. January 2021. Vol. 63, no. 1, p. 103–106. DOI 10.1002/mop.32581.

10. SHI, Yue et al. A Review: Preparation, Performance, and Applications of Silicon Oxynitride Film. *Micromachines*. August 2019. Vol. 10, no. 8, p. 552. DOI 10.3390/mi10080552.

11. PORCEL, Marco A.G. et al. [INVITED] Silicon nitride photonic integration for visible light applications. *Optics & Laser Technology*. April 2019. Vol. 112, p. 299–306. DOI 10.1016/j.optlastec.2018.10.059.

12. XU, Yi et al. Optical Refractive Index Sensors with Plasmonic and Photonic Structures: Promising and Inconvenient Truth. *Advanced Optical Materials*. May 2019. Vol. 7, no. 9, p. 1801433. DOI 10.1002/adom.201801433.

13. HAYASHI, S, NESTERENKO, D V and SEKKAT, and Z. Waveguide-coupled surface plasmon resonance sensor structures: Fano lineshape engineering for ultrahigh-resolution sensing. *Journal of Physics D: Applied Physics*. 19 August 2015. Vol. 48, no. 32, p. 325303. DOI 10.1088/0022-3727/48/32/325303.

14. YANG, Liu et al. Characteristics of multiple Fano resonances in waveguide-coupled surface plasmon resonance sensors based on waveguide theory. *Scientific Reports*. 7 February 2018. Vol. 8, no. 1, p. 2560. DOI 10.1038/s41598-018-20952-7.

15. DU, Wei and ZHAO, Feng. Silicon carbide based surface plasmon resonance waveguide sensor with a bimetallic layer for improved sensitivity. *Materials Letters*. January 2017. Vol. 186, p. 224–226. DOI 10.1016/j.matlet.2016.09.120.

16. DOSTÁLEK, J et al. Surface plasmon resonance biosensor based on integrated optical waveguide. *Sensors and Actuators B: Chemical*. June 2001. Vol. 76, no. 1–3, p. 8–12. DOI 10.1016/S0925-4005(01)00559-7.

17. ČTYROKÝ, J. et al. Theory and modelling of optical waveguide sensors utilising surface plasmon resonance. *Sensors and Actuators B: Chemical*. 25 January 1999. Vol. 54, no. 1–2, p. 66–73. DOI 10.1016/S0925-4005(98)00328-1.

18. WEISS, Martin N. et al. A theoretical investigation of environmental monitoring using surface plasmon resonance waveguide sensors. *Sensors and Actuators A: Physical*. November 1995. Vol. 51, no. 2–3, p. 211–217. DOI 10.1016/0924-4247(95)01208-7.

19. HARRIS, R.D. and WILKINSON, J.S. Waveguide surface plasmon resonance sensors. *Sensors and Actuators B: Chemical*. October 1995. Vol. 29, no. 1–3, p. 261–267. DOI 10.1016/0925-4005(95)01692-9.

20. CHU, Yi-Shin et al. Surface plasmon resonance sensors using silica-on-silicon optical waveguides. *Microwave and Optical Technology Letters*. May 2006. Vol. 48, no. 5, p. 955–957. DOI 10.1002/mop.21531.

21. MISHRA, Satyendra Kumar, ZOU, Bing and CHIANG, Kin Seng. Surface-Plasmon-Resonance Refractive-Index Sensor With Cu-Coated Polymer Waveguide. *IEEE Photonics Technology Letters*. 1 September 2016. Vol. 28, no. 17, p. 1835–1838. DOI 10.1109/LPT.2016.2573322.

22. WALTER, Johanna-Gabriela et al. SPR Biosensor Based on Polymer Multi-Mode Optical Waveguide and Nanoparticle Signal Enhancement. *Sensors*. January 2020. Vol. 20, no. 10, p. 2889. DOI 10.3390/s20102889.

23. LEVY, R. and RUSCHIN, S. SPR waveguide sensor based on transition of modes at abrupt discontinuity. *Sensors and Actuators B: Chemical*. 26 June 2007. Vol. 124, no. 2, p. 459–465. DOI 10.1016/j.snb.2007.01.011.

24. RSoft Photonic Device Tools | Component Design Software | Synopsys. Online. [Accessed 5 July 2023]. Available from: https://www.synopsys.com/photonic-solutions/rsoft-photonic-device-tools/rsoft-products.html

25. MANSURIPUR, Masud, WRIGHT, Ewan M. and FALLAHI, Mahmoud. The Beam Propagation Method. *Optics and Photonics News*. 1 July 2000. Vol. 11, no. 7, p. 42–48. DOI 10.1364/OPN.11.7.000042.

26. PEDROLA, Ginés Lifante. *Beam Propagation Method for Design of Optical Waveguide Devices*. John Wiley & Sons, 2015. ISBN 978-1-119-08338-2.

27. RAHMAN, B.M.A., FERNANDEZ, F.A. and DAVIES, J.B. Review of finite element methods for microwave and optical waveguides. *Proceedings of the IEEE*. October 1991. Vol. 79, no. 10, p. 1442–1448. DOI 10.1109/5.104219.

28. OKAMOTO, Katsunari. *Fundamentals of Optical Waveguides*. Elsevier, 2021. ISBN 978-0-12-815602-5.

29. CHEN, Wai-Kai (ed.). *The electrical engineering handbook*. . Amsterdam ; Boston : Elsevier Academic Press, 2005. ISBN 978-0-12-170960-0. TK145 .E355 2005

30. MOHARAM, M. G. and GAYLORD, T. K. Rigorous coupled-wave analysis of planar-grating diffraction. *JOSA*. 1 July 1981. Vol. 71, no. 7, p. 811–818. DOI 10.1364/JOSA.71.000811.

31. ModePROP™ EME Simulation Tool - RSoft Photonic Device Tools | Synopsys Photonic Solutions. Online. [Accessed 24 February 2023]. Available from: https://www.synopsys.com/photonic-solutions/rsoft-photonic-device-tools/passive-device-modeprop.html

32. REIS, João Carlos R. et al. Refractive Index of Liquid Mixtures: Theory and Experiment. *ChemPhysChem*. 2010. Vol. 11, no. 17, p. 3722–3733. DOI 10.1002/cphc.201000566.

33. ČTYROKÝ, J., HOMOLA, J. and SKALSKÝ, M. Tuning of spectral operation range of a waveguide surface plasmon resonance sensor. *Electronics Letters*. 1997. Vol. 33, no. 14, p. 1246. DOI 10.1049/el:19970814.

34. SAHA, Nabarun et al. Highly Sensitive Refractive Index Sensor Based on Polymer Bragg Grating: A Case Study on Extracellular Vesicles Detection. *Biosensors*. June 2022. Vol. 12, no. 6, p. 415. DOI 10.3390/bios12060415.

35. STEGLICH, Patrick et al. CMOS-Compatible Silicon Photonic Sensor for Refractive Index Sensing Using Local Back-Side Release. *IEEE Photonics Technology Letters*. October 2020. Vol. 32, no. 19, p. 1241–1244. DOI 10.1109/LPT.2020.3019114.

36. FARUQUE, Md. Omar, AL MAHMUD, Rabiul and SAGOR, Rakibul Hasan. Highly Sensitive Plasmonic Refractive Index Sensor Using Doped Silicon: an Alternative to MIM Structures. *Plasmonics*. 1 February 2022. Vol. 17, no. 1, p. 203–211. DOI 10.1007/s11468-021-01516-4.

37. KUMAR, Manoj, KUMAR, Arun and TRIPATHI, Saurabh Mani. Optical waveguide biosensor based on modal interference between surface plasmon modes. *Sensors and Actuators B: Chemical*. 1 May 2015. Vol. 211, p. 456–461. DOI 10.1016/j.snb.2015.01.088.

38. CHEN, Xinzhong et al. Modern Scattering-Type Scanning Near-Field Optical Microscopy for Advanced Material Research. *Advanced Materials*. June 2019. Vol. 31, no. 24, p. 1804774. DOI 10.1002/adma.201804774.

Zoznam publikačnej činnosti

Autor: Feiler, Martin

1) Výstupy kategórie A+, A, A- a B, spolu: 24
2) Výstupy kategórie A+ a A, spolu: 3
3) Počet publikácii vo WoS/SCOPUS: 5 (z toho 4 WoS a 5 SCOPUS)

Kategória A+: 3

V3 Vedecký výstup publikačnej činnosti z časopisu

V3_01 ESFAHANI, Niloofar Ebrahimzadeh [50 %] - KOVÁČ, Jaroslav jr. [30 %] - KOVÁČOVÁ, Soňa [10 %] - **FEILER, Martin** [10 %]. Plasmonic properties of the metal nanoparticles (NPs) on a metal mirror separated by an ultrathin oxide layer. In *Photonics*. Vol. 10, iss. 1 (2023), Art. no. 78 [12] s. ISSN 2304-6732 (2021: 2.536 - IF, Q3 - JCR Best Q, 0.558 - SJR, Q2 - SJR Best Q). V databáze: DOI: 10.3390/photonics10010078 ; SCOPUS: 2-s2.0-85146819985.
Typ výstupu: článok; Výstup: zahraničný; Kategória publikácie do 2021: ADC

V3_02 **FEILER, Martin** [65 %] - ZIMAN, Martin [15 %] - KOVÁČ, Jaroslav jr. [10 %] - KUZMA, Anton [5 %] - UHEREK, František [5 %]. Design of Optimal SPR-Based Multimode Waveguide Sensor for a Wide Range of Liquid Analytes. In *Photonics*. Vol. 10, iss. 6 (2023), Art. no. 618 [10] s. ISSN 2304-6732 (2021: 2.536 - IF, Q3 - JCR Best Q, 0.558 - SJR, Q2 - SJR Best Q). V databáze: DOI: 10.3390/photonics10060618 ; WOS: 001017896200001 ; CC: 001017896200001 ; SCOPUS: 2-s2.0-85163794308.
Typ výstupu: článok; Výstup: zahraničný; Kategória publikácie do 2021: ADC

V3_03 ZIMAN, Martin [55 %] - **FEILER, Martin** [15 %] - MIZERA, Tomáš [15 %] - KUZMA, Anton [5 %] - PUDIŠ, Dušan [5 %] - UHEREK, František [5 %]. Design of a power splitter based on a 3D MMI coupler at the fibre-tip. In *Electronics*. Vol. 11, iss. 18 (2022), Art. no. 2815 [11] s. ISSN 2079-9292 (2022: 2.900 - IF, Q2 - JCR Best Q, 0.628 - SJR, Q2 - SJR Best Q). V databáze: DOI: 10.3390/electronics11182815 ; SCOPUS: 2-s2.0-85138694363 ; WOS: 000856492300001 ; CC: 000856492300001.
Typ výstupu: článok; Výstup: zahraničný; Kategória publikácie do 2021: ADC

Kategória A-: 2

V2 Vedecký výstup publikačnej činnosti ako časť editovanej knihy alebo zborníka

V2_01 CHLPÍK, Juraj [25 %] - KOVÁČOVÁ, Soňa [10 %] - PODLUCKÝ, Ľuboš [10 %] - ZIMAN, Martin [10 %] - **FEILER, Martin** [10 %] - KOTOROVÁ, Soňa [10 %] - KOVÁČ, Jaroslav jr. [10 %] - VÁRY, Tomáš [10 %] - CIRÁK, Július [5 %]. Total internal reflection ellipsometry of Au/SiOxNy waveguide structures for sensor applications. In *APCOM 2022 : 27th International conference on applied physics of condensed matter. Štrbské Pleso, Slovak Republic. June 22-24, 2022*. 1. ed. Melville : AIP Publishing, 2023, Art. no. 030005 [7] s. ISBN 978-0-7354-4479-9. V databáze: DOI: 10.1063/5.0135889 ; SCOPUS: 2-s2.0-85160269603.
Typ výstupu: príspevok z podujatia; Výstup: domáci; Kategória publikácie do 2021: AFD

V2_02 LETTRICHOVÁ, Ivana [27 %] - PUDIŠ, Dušan [20 %] - JANDURA, Daniel [15 %] - GAŠO, Peter [10 %] - **FEILER, Martin** [10 %] - KOVÁČ, Jaroslav jr. [10 %] - LAURENČÍKOVÁ, Agáta [5 %] - ZIMAN, Martin [3 %]. IP-Dip inverted pyramids for application in SERS. In *22nd Polish-Slovak-Czech Optical Conference on Wave and Quantum Aspects of Contemporary Optics : Wojanow, Poland. September 5-9, 2022*. Bellingham : SPIE, 2022, Art. no. 125020P [6] s. ISSN 0277-786X. ISBN 978-1-510-66111-0 (2022: 0.166 - SJR). V databáze: DOI: 10.1117/12.2664208 ; SCOPUS: 2-s2.0-85145359283 ; WOS: 000920988700024.
Typ výstupu: príspevok z podujatia; Výstup: zahraničný; Kategória publikácie do 2021: AFC

Kategória B: 17

V2_03 ESFAHANI, Niloofar Ebrahimzadeh [70 %] - **FEILER, Martin** [20 %] - KOVÁČOVÁ, Soňa [5 %] - KOVÁČ, Jaroslav jr. [5 %]. Strong field enhancement of the film coupled nanoparticle plasmonic structure. In *ADEPT 2022 : 10th International conference on advances in electronic and photonic technologies. Tatranská Lomnica, Slovakia. June 20-24, 2022*. 1. vyd. Žilina : Vydavateľstvo EDIS, 2022, S. 97-100. ISBN 978-80-554-1884-1.
Typ výstupu: príspevok z podujatia; Výstup: domáci; Kategória publikácie do 2021: AFD

V2_04 **FEILER, Martin** [50 %] - KUZMA, Anton [20 %] - UHEREK, František [10 %] - KOVÁČ, Jaroslav jr. [20 %]. Transmission of light through subwavelength slits between metallic strips. In *ADEPT 2020 : 8th International conference on advances in electronic and photonic technologies. Nový Smokovec, Slovakia. September 14-17, 2020.* 1. vyd. Žilina : Vydavateľstvo EDIS, 2020, S. 107-110. ISBN 978-80-554-1735-6.
Typ výstupu: príspevok z podujatia; Výstup: domáci; Kategória publikácie do 2021: AFD

V2_05 **FEILER, Martin** [35 %] - KUZMA, Anton [20 %] - URBANCOVÁ, Petra [15 %] - UHEREK, František [15 %] - GORAUS, Matej [15 %]. Investigation of woodpile structure by plane-wave expansion simulation method. In *ADEPT 2020 : 8th International conference on advances in electronic and photonic technologies. Nový Smokovec, Slovakia. September 14-17, 2020*. 1. vyd. Žilina : Vydavateľstvo EDIS, 2020, S. 139-142. ISBN 978-80-554-1735-6.
Typ výstupu: príspevok z podujatia; Výstup: domáci; Kategória publikácie do 2021: AFD

V2_06 **FEILER, Martin** [50 %] - ZIMAN, Martin [15 %] - KUZMA, Anton [15 %] - KOVÁČ, Jaroslav jr. [10 %] - UHEREK, František [10 %]. Design and simulation of optical waveguide sensor based on SiN material platform utilising surface plasmon resonance. In *ADEPT 2021 : 9th International conference on advances in electronic and photonic technologies. Podbanské, Slovakia. September 20-23.2021*. 1. vyd. Žilina : Vydavateľstvo EDIS, 2021, S. 95-98. ISBN 978-80-554-1806-3.
Typ výstupu: príspevok z podujatia; Výstup: domáci; Kategória publikácie do 2021: AFD

V2_07 **FEILER, Martin** [30 %] - KUZMA, Anton [25 %] - PUDIŠ, Dušan [20 %] - URBANCOVÁ, Petra [15 %] - UHEREK, František [10 %]. Near-field probes based on nanocone and nanopyramid – design and simulation. In *ADEPT 2021 : 9th International conference on advances in electronic and photonic technologies. Podbanské, Slovakia. September 20-23.2021*. 1. vyd. Žilina : Vydavateľstvo EDIS, 2021, S. 223-226. ISBN 978-80-554-1806-3.
Typ výstupu: príspevok z podujatia; Výstup: domáci; Kategória publikácie do 2021: AFD

V2_08 **FEILER, Martin** [65 %] - ZIMAN, Martin [20 %] - KUZMA, Anton [5 %] - KOVÁČ, Jaroslav jr. [5 %] - UHEREK, František [5 %]. Design and simulation of optical grating coupler on SiON material platform. In *ELITECH´22 [elektronický zdroj] : 24th Conference of Doctoral Students. Bratislava, Slovakia. June 1, 2022*. 1. ed. Bratislava : Vydavateľstvo Spektrum STU, 2022, [4] s. ISBN 978-80-227-5192-6.
Typ výstupu: príspevok z podujatia; Výstup: domáci; Kategória publikácie do 2021: AFD

V2_09 **FEILER, Martin** [60 %] - ZIMAN, Martin [15 %] - KUZMA, Anton [10 %] - KOVÁČ, Jaroslav jr. [10 %] - UHEREK, František [5 %]. Design and simulation of grating for fiber-to-chip coupling on SiON material platform. In *ADEPT 2022 : 10th International conference on advances in electronic and photonic technologies. Tatranská Lomnica, Slovakia. June 20-24, 2022*. 1. vyd. Žilina : Vydavateľstvo EDIS, 2022, S. 101-104. ISBN 978-80-554-1884-1.
Typ výstupu: príspevok z podujatia; Výstup: domáci; Kategória publikácie do 2021: AFD

V2_10 **FEILER, Martin** [65 %] - ZIMAN, Martin [15 %] - KOVÁČ, Jaroslav jr. [10 %] - KUZMA, Anton [10 %]. Single-mode waveguide based SPR refractive index sensor for lab-on-chip applications. In *ADEPT 2023 : 11th International conference on advances in electronic and photonic technologies. Podbanské, Slovakia. June 12-15, 2023*. 1. vyd. Žilina : Vydavateľstvo EDIS, 2023, S. 75-78. ISBN 978-80-554-1977-0.
Typ výstupu: príspevok z podujatia; Výstup: domáci; Kategória publikácie do 2021: AFD

V2_11 HAUSNER, Michal [50 %] - **FEILER, Martin** [25 %] - PODLUCKÝ, Ľuboš [15 %] - KOVÁČOVÁ, Soňa [5 %] - KOVÁČ, Jaroslav jr. [5 %]. Transmision measurement of SiON waveguide structures with plasmonic sensor layer. In *ADEPT 2023 : 11th International conference on advances in electronic and photonic technologies. Podbanské, Slovakia. June 12-15, 2023*. 1. vyd. Žilina : Vydavateľstvo EDIS, 2023, S. 79-82. ISBN 978-80-554-1977-0.
Typ výstupu: príspevok z podujatia; Výstup: domáci; Kategória publikácie do 2021: AFD

V2_12 PODLUCKÝ, Ľuboš [55 %] - KOVÁČOVÁ, Soňa [15 %] - HAUSNER, Michal [10 %] - **FEILER, Martin** [10 %] - ZIMANOVÁ, Jana [5 %] - KOVÁČ, Jaroslav jr. [5 %]. SiON photonic Grating Couplers Fabrication. In *ADEPT 2023 : 11th International conference on advances in electronic and photonic technologies. Podbanské, Slovakia. June 12-15, 2023*. 1. vyd. Žilina : Vydavateľstvo EDIS, 2023, S. 202-205. ISBN 978-80-554-1977-0.
Typ výstupu: príspevok z podujatia; Výstup: domáci; Kategória publikácie do 2021: AFD

V2_13 PUDIŠ, Dušan [25 %] - KUZMA, Anton [20 %] - MANIAKOVÁ, P. [15 %] - **FEILER, Martin** [15 %] - JANDURA, Daniel [15 %] - GORAUS, Matej [10 %]. Near-field probes based on nanocones and nanopyramide. In *Optics, photonics and lasers : 5th International conference. Tenerife, Spain. May 18-20, 2022*. Barcelona : IFSA Publishing, 2022, S. 65-66. ISBN 978-84-09-40460-5.
Typ výstupu: príspevok z podujatia; Výstup: domáci; Kategória publikácie do 2021: AFC

V2_14 ŠUŠLIK, Ľuboš [40 %] - GAŠO, Peter [20 %] - **FEILER, Martin** [20 %] - JANDURA, Daniel [10 %] - KUZMA, Anton [10 %]. 3D photonic structures for optoelectronics applications. In *ADEPT 2021 : 9th International conference on advances in electronic and photonic technologies. Podbanské, Slovakia. September 20-23.2021*. 1. vyd. Žilina : Vydavateľstvo EDIS, 2021, S. 247-250. ISBN 978-80-554-1806-3.
Typ výstupu: príspevok z podujatia; Výstup: domáci; Kategória publikácie do 2021: AFD

V2_15 ZIMAN, Martin [50 %] - **FEILER, Martin** [15 %] - KUZMA, Anton [15 %] - KOVÁČ, Jaroslav jr. [10 %] - UHEREK, František [10 %]. Simulations of surface plasmon resonance based fiber probe. In *ADEPT 2021 : 9th International conference on advances in electronic and photonic technologies. Podbanské, Slovakia. September 20-23.2021*. 1. vyd. Žilina: Vydavateľstvo EDIS, 2021, S. 175-178. ISBN 978-80-554-1806-3.
Typ výstupu: príspevok z podujatia; Výstup: domáci; Kategória publikácie do 2021: AFD

V2_16 ZIMAN, Martin [40 %] - **FEILER, Martin** [15 %] - UHEREK, František [10 %] - MIZERA, Tomáš [15 %] - KUZMA, Anton [10 %] - JAGELKA, Martin [10 %]. Design and simulation of 3D MMI splitter based on polymer. In *ELITECH´22 [elektronický zdroj] : 24th Conference of Doctoral Students. Bratislava, Slovakia. June 1, 2022*. 1. ed. Bratislava : Vydavateľstvo Spektrum STU, 2022, [5] s. ISBN 978-80-227-5192-6.
Typ výstupu: príspevok z podujatia; Výstup: domáci; Kategória publikácie do 2021: AFD

V2_17 ZIMAN, Martin [60 %] - KUZMA, Anton [10 %] - **FEILER, Martin** [10 %] - MIZERA, Tomáš [10 %] - PUDIŠ, Dušan [5 %] - UHEREK, František [5 %]. Design and simulations of 1xN polymer-based MMI splitters. In *ADEPT 2022 : 10th International conference on advances in electronic and photonic technologies. Tatranská Lomnica, Slovakia. June 20-24, 2022*. 1. vyd. Žilina : Vydavateľstvo EDIS, 2022, S. 238-241. ISBN 978-80-554-1884-1.
Typ výstupu: príspevok z podujatia; Výstup: domáci; Kategória publikácie do 2021: AFD

V2_18 ZIMAN, Martin [20 %] - **FEILER, Martin** [20 %] - MIZERA, Tomáš [20 %] - KUZMA, Anton [20 %] - UHEREK, František [20 %]. Návrh a simulácie deliča výkonu založeného na 3D MMI člene. In *Fotonika 2022 : 17. výročný vedecký seminár Medzinárodného laserového centra CVTI SR. Bratislava, Slovakia. 07. december 2022*. Bratislava : Medzinárodné laserové centrum, 2022, S. 111-115. ISBN 978-80-8240-033-8.
Typ výstupu: príspevok z podujatia; Výstup: domáci; Kategória publikácie do 2021: AFD

V2_19 ZIMAN, Martin [60 %] - **FEILER, Martin** [15 %] - KOVÁČ, Jaroslav jr. [15 %] - DONOVAL, Daniel [5 %] - KUZMA, Anton [5 %]. Simulation investigation of fibre-tip sensor prepared by DLW printing. In *ADEPT 2023 : 11th International conference on advances in electronic and photonic technologies. Podbanské, Slovakia. June 12-15, 2023*. 1. vyd. Žilina : Vydavateľstvo EDIS, 2023, S. 123-126. ISBN 978-80-554-1977-0.
Typ výstupu: príspevok z podujatia; Výstup: domáci; Kategória publikácie do 2021: AFD

Ostatné publikácie: 2

V1 Vedecký výstup publikačnej činnosti ako celok

V1_01 **FEILER, Martin** [25 %] - (zost.) - ZIMAN, Martin [25 %] - (zost.) - KOVÁČOVÁ, Soňa [25 %] - (zost.) - KOVÁČ, Jaroslav jr. [25 %] - (zost.). *ADEPT 2022 : 10th International conference on advances in electronic and photonic technologies. Tatranská Lomnica, Slovakia. June 20-24, 2022*. 1. vyd. Žilina : Vydavateľstvo EDIS, 2022. 274 s. ISBN 978-80-554-1884-1.
Typ výstupu: zborník; Výstup: domáci; Kategória publikácie do 2021: FAI

V1_02 KOVÁČ, Jaroslav jr. [25 %] - (zost.) - CHYMO, Filip [25 %] - (zost.) - **FEILER, Martin** [25 %] - (zost.) - JANDURA, Daniel [25 %] - (zost.). *ADEPT 2020 : 8th International conference on advances in electronic and photonic technologies. Nový Smokovec, Slovakia. September 14-17, 2020*. 1. vyd. Žilina : Vydavateľstvo EDIS, 2020. 192 s. ISBN 978-80-554-1735-6.
Typ výstupu: zborník; Kategória publikácie do 2021: FAI

Štatistika: kategória publikačnej činnosti od 2022

V1	Vedecký výstup publikačnej činnosti ako celok	2
V2	Vedecký výstup publikačnej činnosti ako časť editovanej knihy alebo zborníka	19
V3	Vedecký výstup publikačnej činnosti z časopisu	3
Súčet		**24**

Štatistika: kategória publikačnej činnosti do 2021

ADC	Vedecké práce v zahraničných karentovaných časopisoch	3
AFC	Publikované príspevky na zahraničných vedeckých konferenciách	2
AFD	Publikované príspevky na domácich vedeckých konferenciách	17
FAI	Redakčné a zostavovateľské práce knižného charakteru (bibliografie, encyklopédie, katalógy, slovníky, zborníky...)	2
Súčet		**24**

Ohlasy na publikácie autora

Citácie, spolu: 2 (Z toho registrované vo WoS alebo SCOPUS : 2)

Publikácia:

ESFAHANI, Niloofar Ebrahimzadeh [50 %] - KOVÁČ, Jaroslav jr. [30 %] - KOVÁČOVÁ, Soňa [10 %] - **FEILER, Martin** [10 %]. Plasmonic properties of the metal nanoparticles (NPs) on a metal mirror separated by an ultrathin oxide layer. In *Photonics*. Vol. 10, iss. 1 (2023), Art. no. 78 [12] s. ISSN 2304-6732 (2021: 2.536 - IF, Q3 - JCR Best Q, 0.558 - SJR, Q2 - SJR Best Q). V databáze: DOI: 10.3390/photonics10010078 ; SCOPUS: 2-s2.0-85146819985.

Citovaná v:

LIU, Wenjie, et al. Facile Preparation of Au–Ag Composite Nanostructure for High-Sensitive and Uniform Surface-Enhanced Raman Spectroscopy. In: *Photonics*. MDPI, 2023. p. 354.

Publikácia:

FEILER, Martin [65 %] - ZIMAN, Martin [15 %] - KOVÁČ, Jaroslav jr. [10 %] - KUZMA, Anton [5 %] - UHEREK, František [5 %]. Design of Optimal SPR-Based Multimode Waveguide Sensor for a Wide Range of Liquid Analytes. In *Photonics*. Vol. 10, iss. 6 (2023), Art. no. 618 [10] s. ISSN 2304-6732 (2021: 2.536 - IF, Q3 - JCR Best Q, 0.558 - SJR, Q2 - SJR Best Q). V databáze: DOI: 10.3390/photonics10060618 ; WOS: 001017896200001 ; CC: 001017896200001 ; SCOPUS: 2-s2.0-85163794308..

Citovaná v:

SHAHBAZ, Muhammad; BUTT, Muhammad A.; PIRAMIDOWICZ, Ryszard. A Concise Review of the Progress in Photonic Sensing Devices. In: *Photonics*. MDPI, 2023. p. 698.

Author: Ing. Martin Feiler

Thesis title: Photonic structures for sensor applications

Volume: 12 units

The dissertation thesis and its abstract are stored at the Faculty of Electrical Engineering and Information Technology of STU in Bratislava